

**Measurement of the  $\alpha$  Energy Spectrum from  
8B and Determination of the Shape of the  
 $\nu$  Spectrum**

**C.Ortiz**

**A. Garcia**

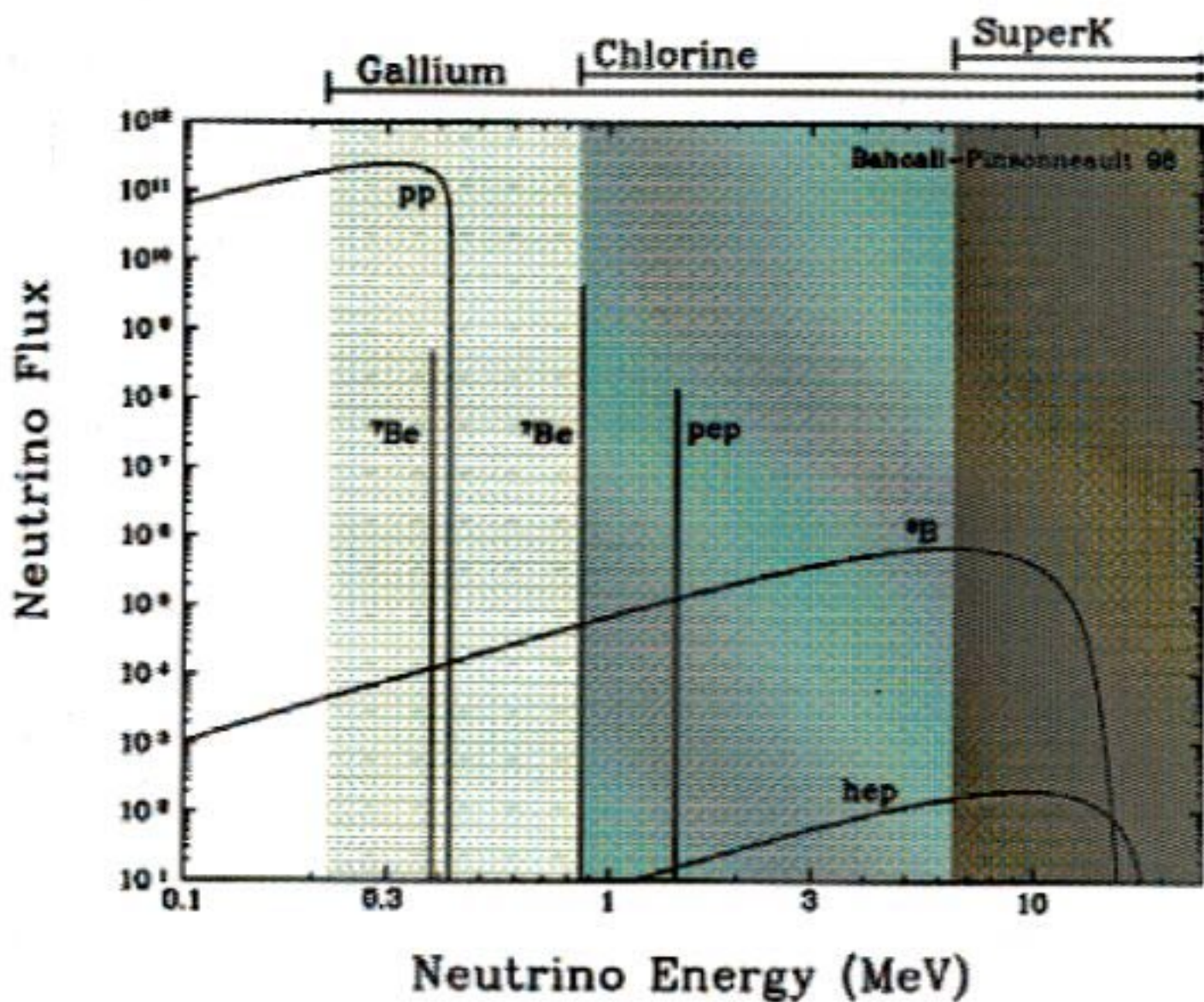
**M. Bhattacharya**

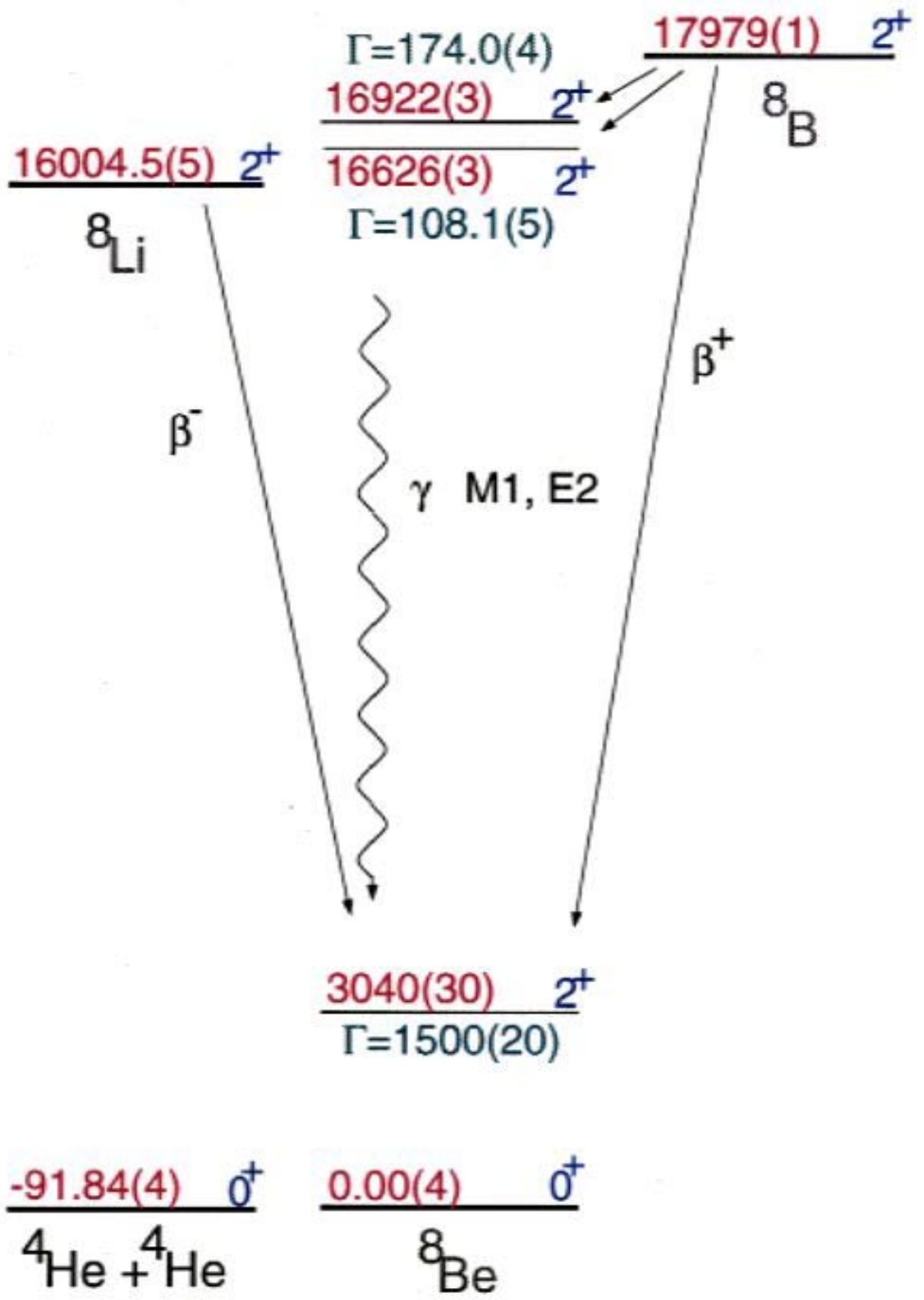
**A. Komives**

**R. Waltz**

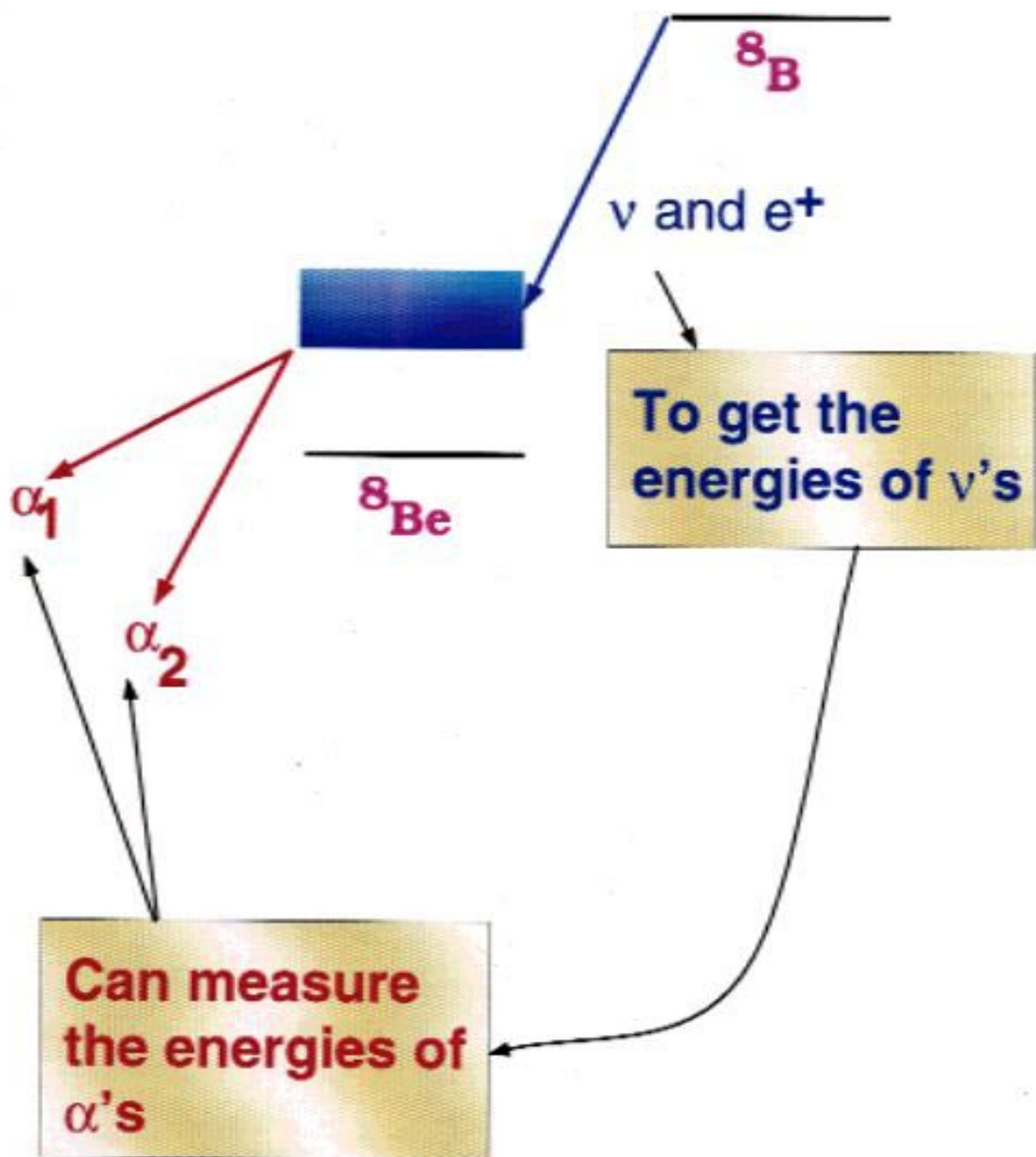
**University of  
Notre Dame**

# SuperK, SNO, ICARUS... will look at distortions of the $8B \nu$ spectrum





# High-energy $\nu$ 's come from ${}^8\text{B}$



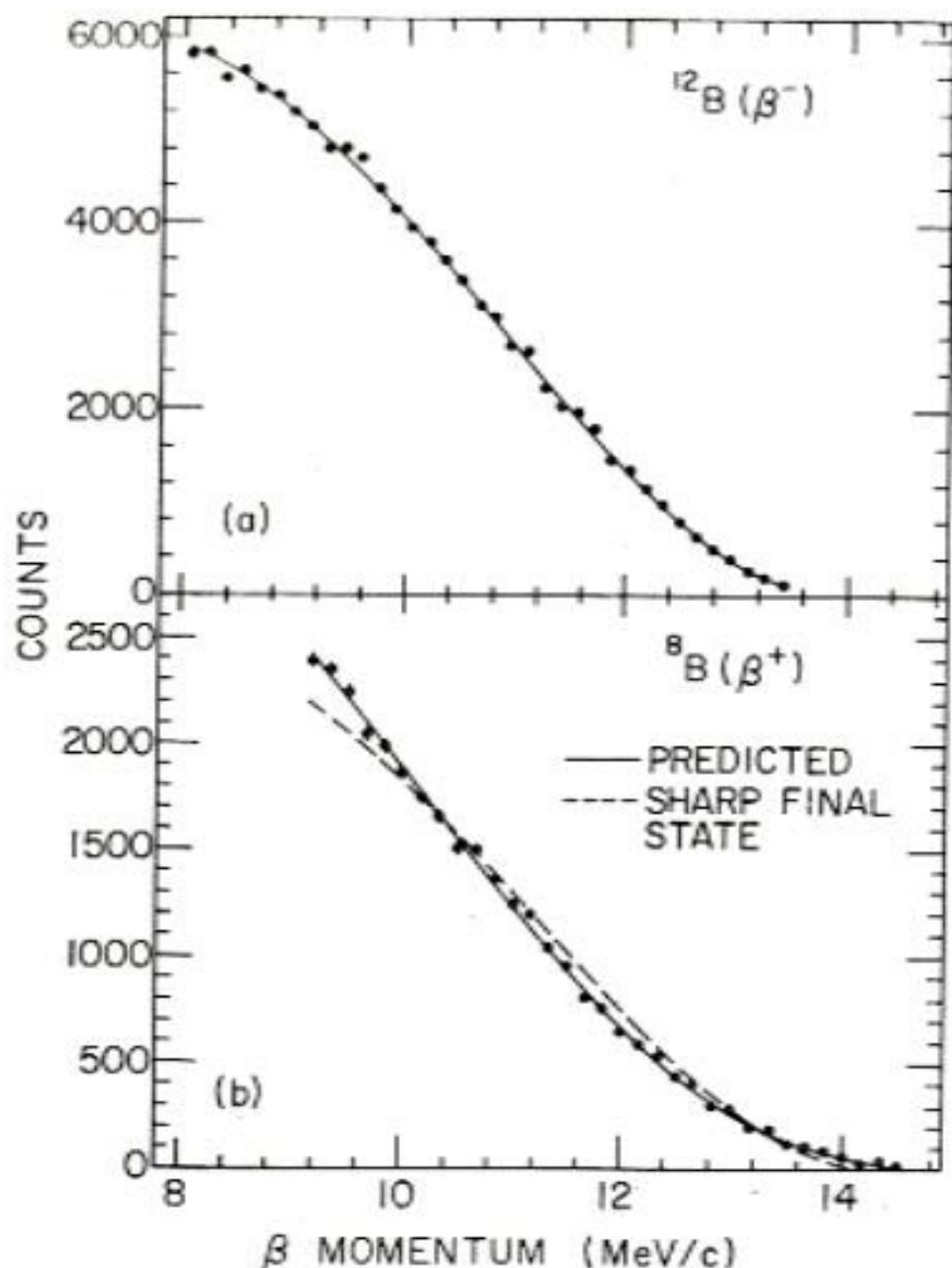


FIG. 2. Measured  $\beta$  momentum spectra. The error bars, where not shown, are smaller than the size of the points. (a) The  $\beta^-$  spectrum of  $^{12}\text{B}$  used to calibrate the spectrometer. A fit is performed to obtain the calibration parameter  $R_0$  (see Ref. 15). (b) The  $\beta^+$  spectrum of  $^8\text{B}$ . The solid line is the predicted spectrum which gives the best agreement (see Table I). The dashed line shows a normal allowed spectrum for a hypothetical sharp final state at  $E_x \approx 3$  MeV in  $^8\text{Be}$ .

when both recoil order terms and radiative corrections are

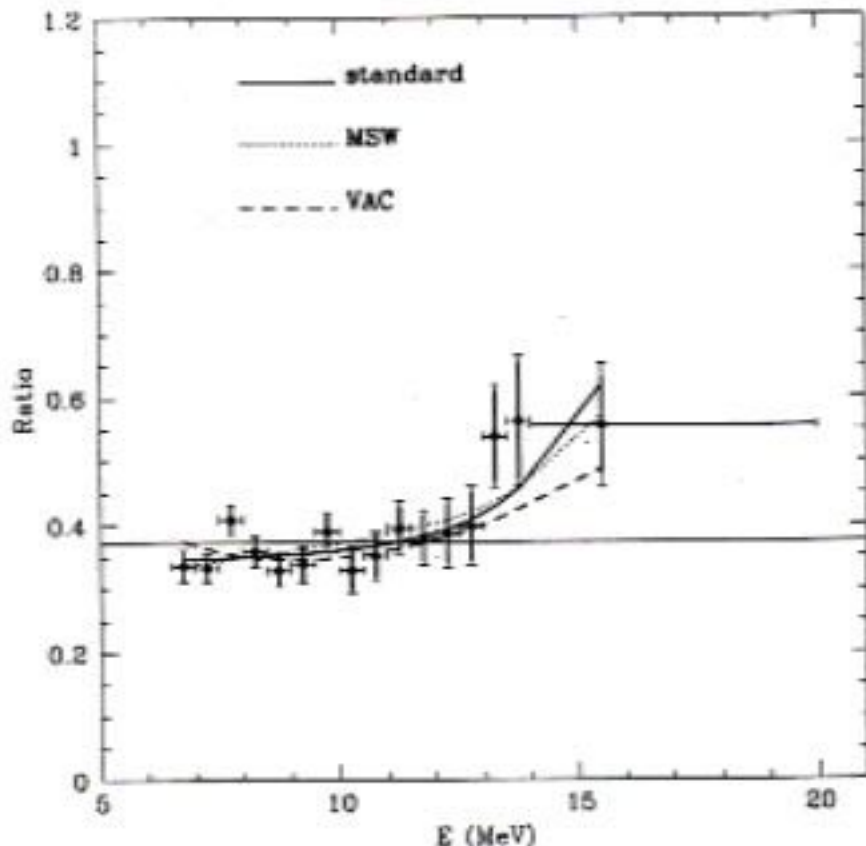


Fig. 1. Combined  ${}^8\text{B}$  plus  $h\nu p$  energy spectrum. The total flux of  $h\nu p$  neutrinos was varied to obtain the best-fit for each scenario. The figure shows the Ratio of the measured [1] to the calculated number of events with electron recoil energy,  $E$ . The measured points were reported by the SuperKamiokande collaboration at Neutrino 98[1]. The calculated curves are global fits to all of the data, the chlorine [20], GALLEX [21], SAGE [22], and SuperKamiokande [1] total event rates, the Superkamiokande [1] energy spectrum, and the SuperKamiokande [1] Day-Night asymmetry. The calculations follow the precepts of BKS98 [23] for the best-fit global solutions for a standard 'no-oscillation' energy spectrum, as well as MSW and vacuum neutrino oscillation solutions. The horizontal line at Ratio = 0.37 represents the ratio of the total event rate measured by SuperKamiokande to the predicted event rate[9] with no oscillations and only  ${}^8\text{B}$  neutrinos.

For vacuum oscillations, the value of  $\alpha$  corresponding to the global  $\chi^2_{\min}$  does not depend strongly on  $\Delta m^2$  and  $\sin^2 2\theta$  within the acceptable region. The improvement in the C.L. for acceptance increases from 6% to 15% when an arbitrary  $h\nu p$  flux is considered.

The best-fit global MSW solution with an arbitrary  $h\nu p$  flux has neutrino parameters given by  $\Delta m^2 = 5.4 \times 10^{-6} \text{eV}^2$  and  $\sin^2 2\theta = 5.0 \times 10^{-3}$ , which

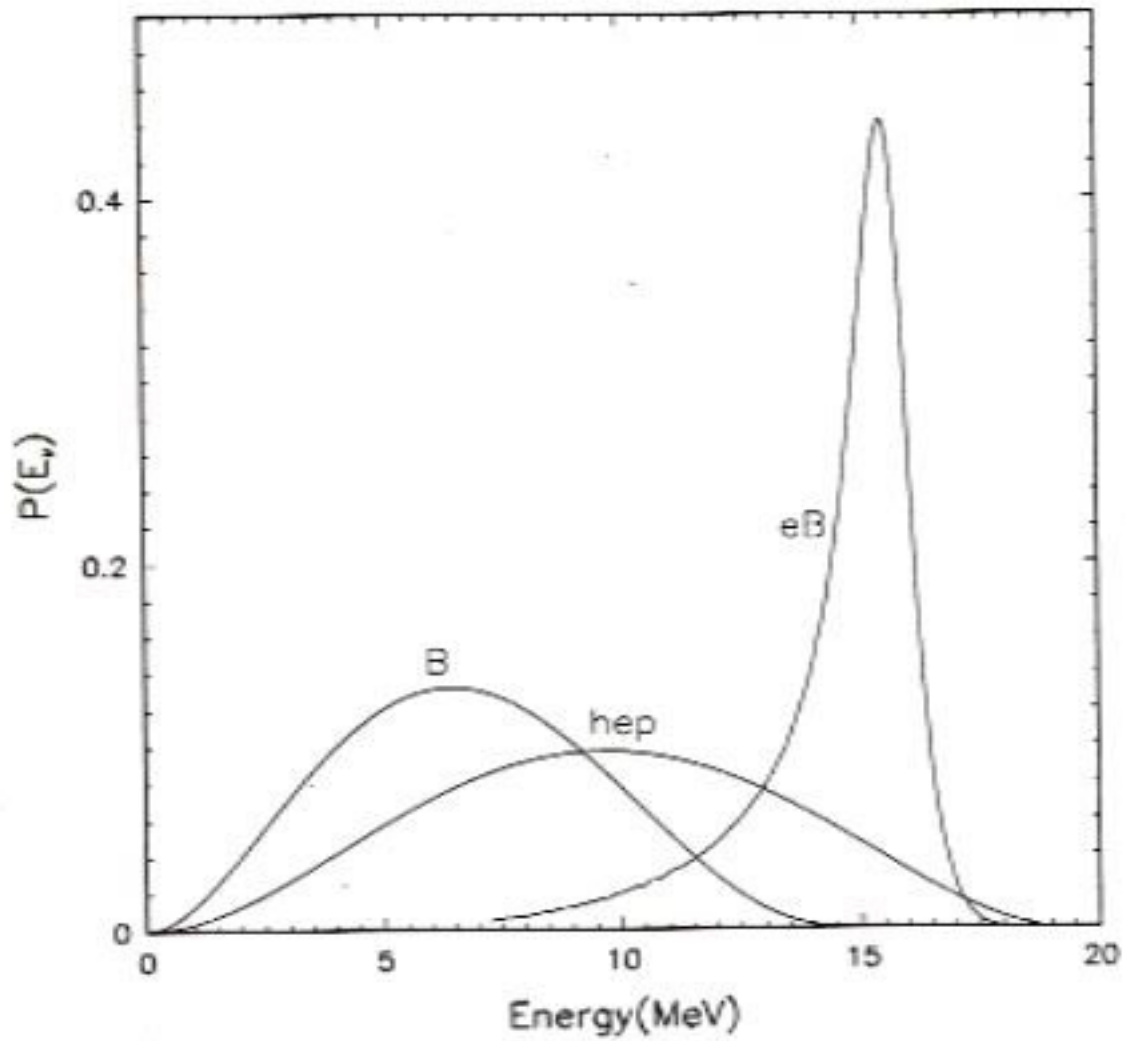


Figure 1: Normalized energy spectra of  $^8B$ , hep and eB neutrinos.

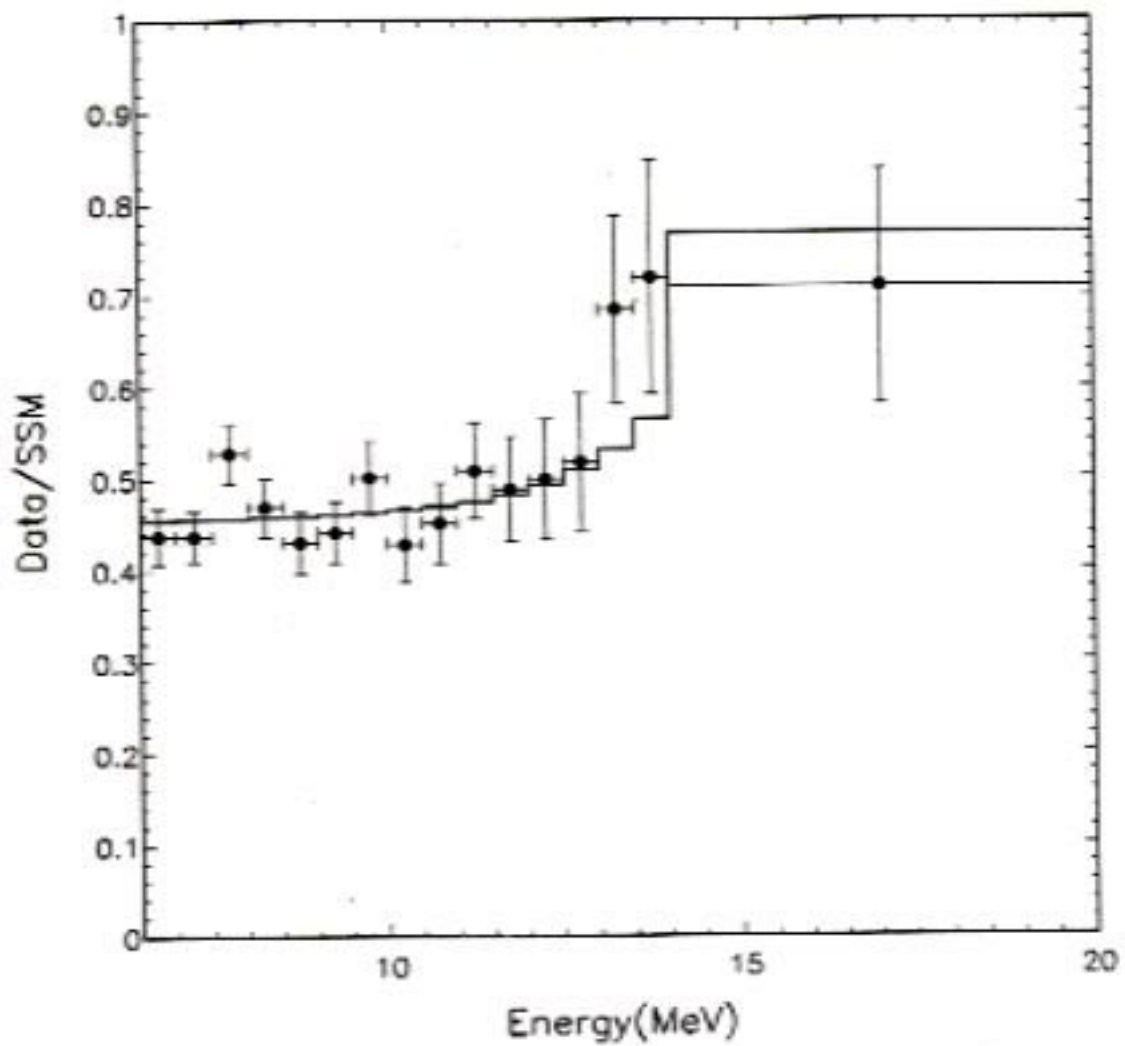


Figure 3: Observed electron energy spectrum normalized to SSM expectations (dots).  
The solid line is the prediction for  $\Phi_e = 1.1 \times 10^4 \text{ cm}^{-2} \text{ s}^{-1}$ .



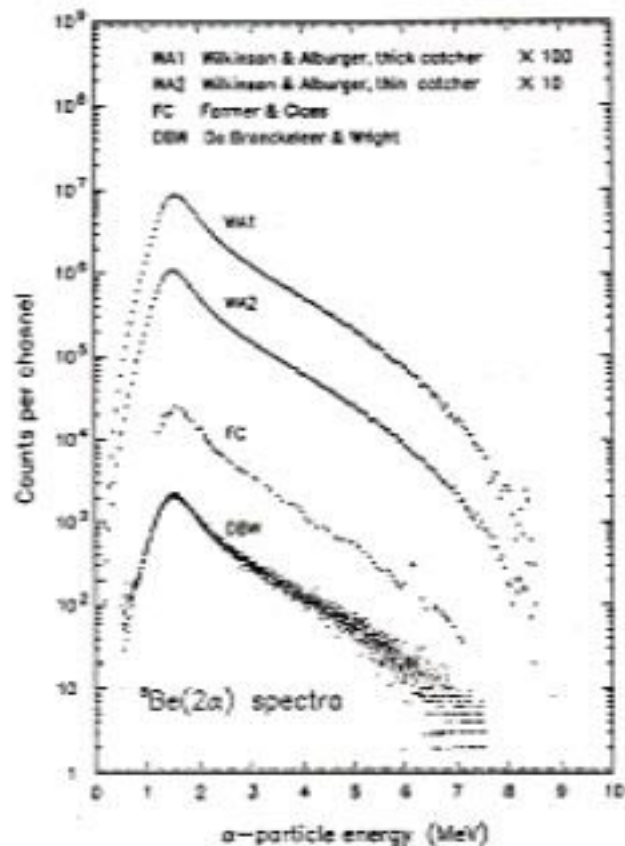


FIG. 2. Compilation of  ${}^8\text{Be}(2\alpha)$  decay data. The bias widths are different for different experiments. The data WA1 and WA2 are shifted on the vertical axis.

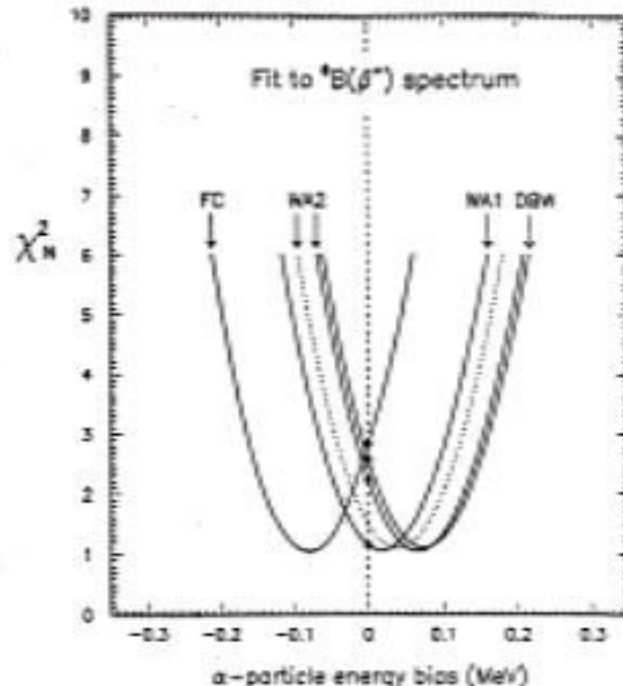


FIG. 3. Values of the normalized chi square in a fit to the experimental positron spectrum, using the input alpha decay data of Fig. 2, with an allowance for a possible bias,  $b$ , in the detected alpha particle energy. The curves are remarkably similar, modulo a constant bias.

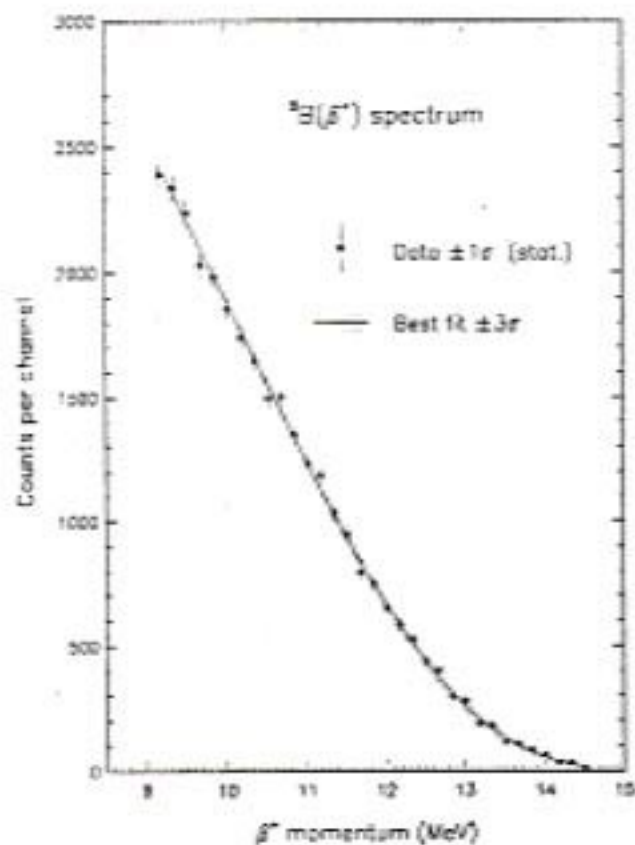


FIG. 4. Experimental data on the positron spectrum, together with the best fit and the  $\pm 3\sigma$  fits, corresponding to WA1 alpha decay data within the bias range  $b = 0.025 \pm 0.056$  MeV.

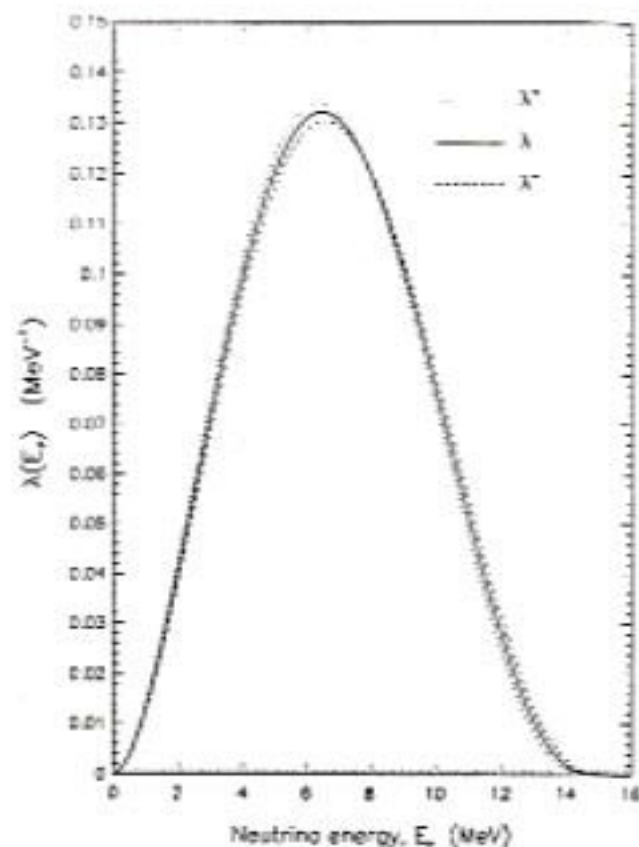
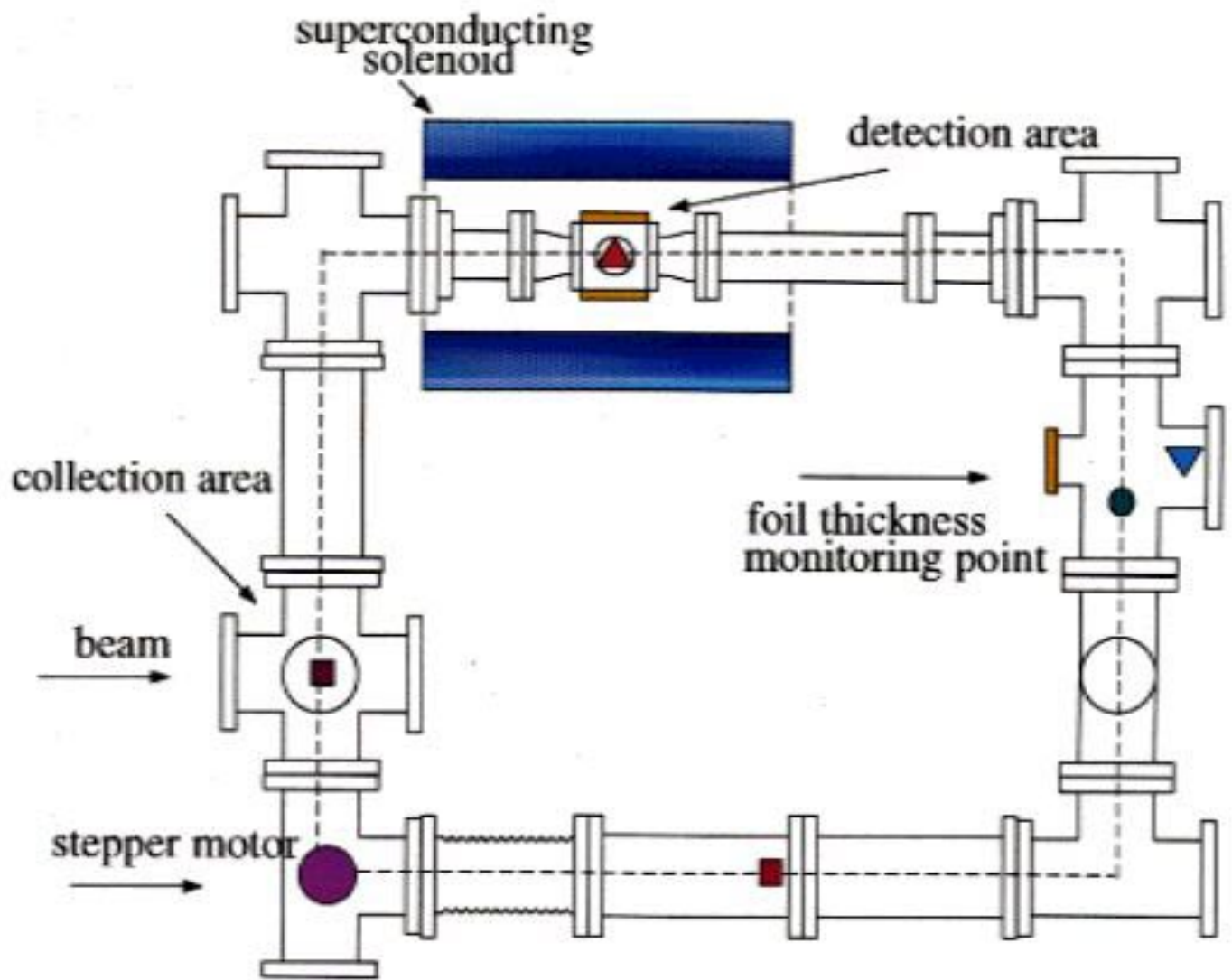
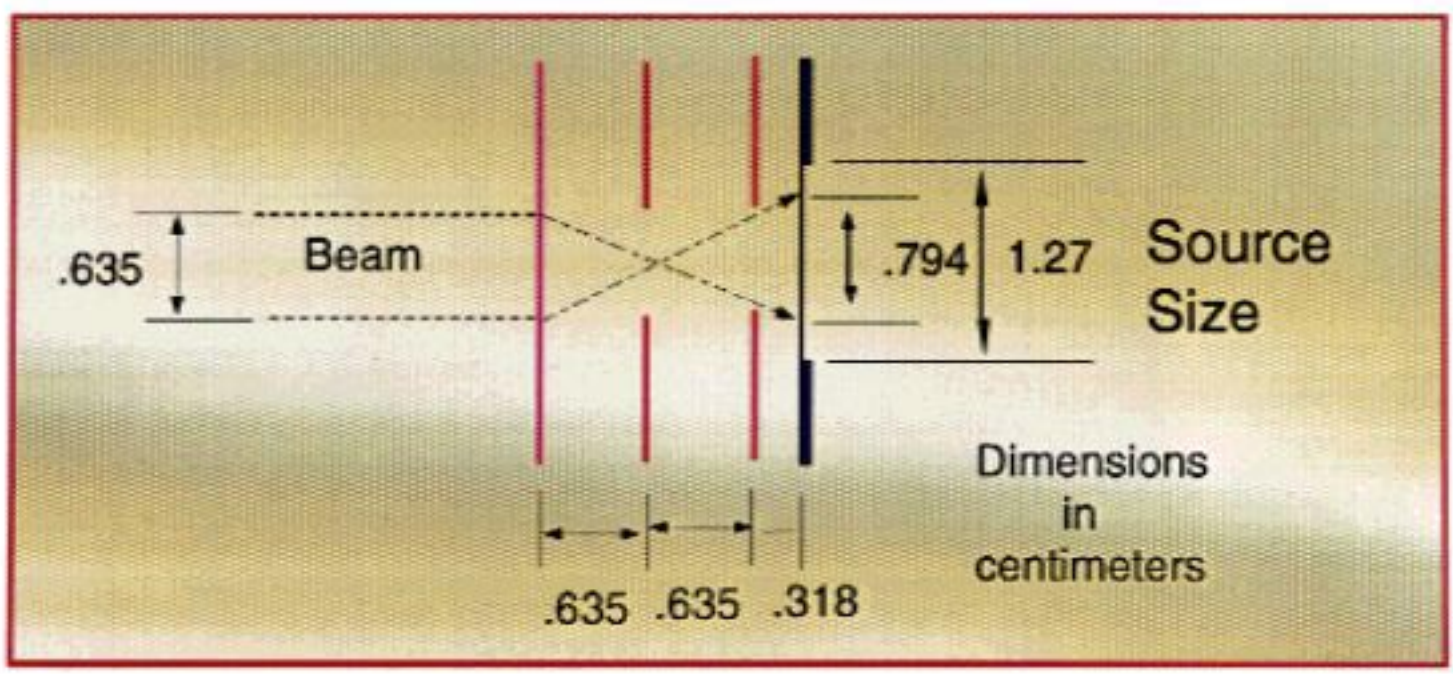
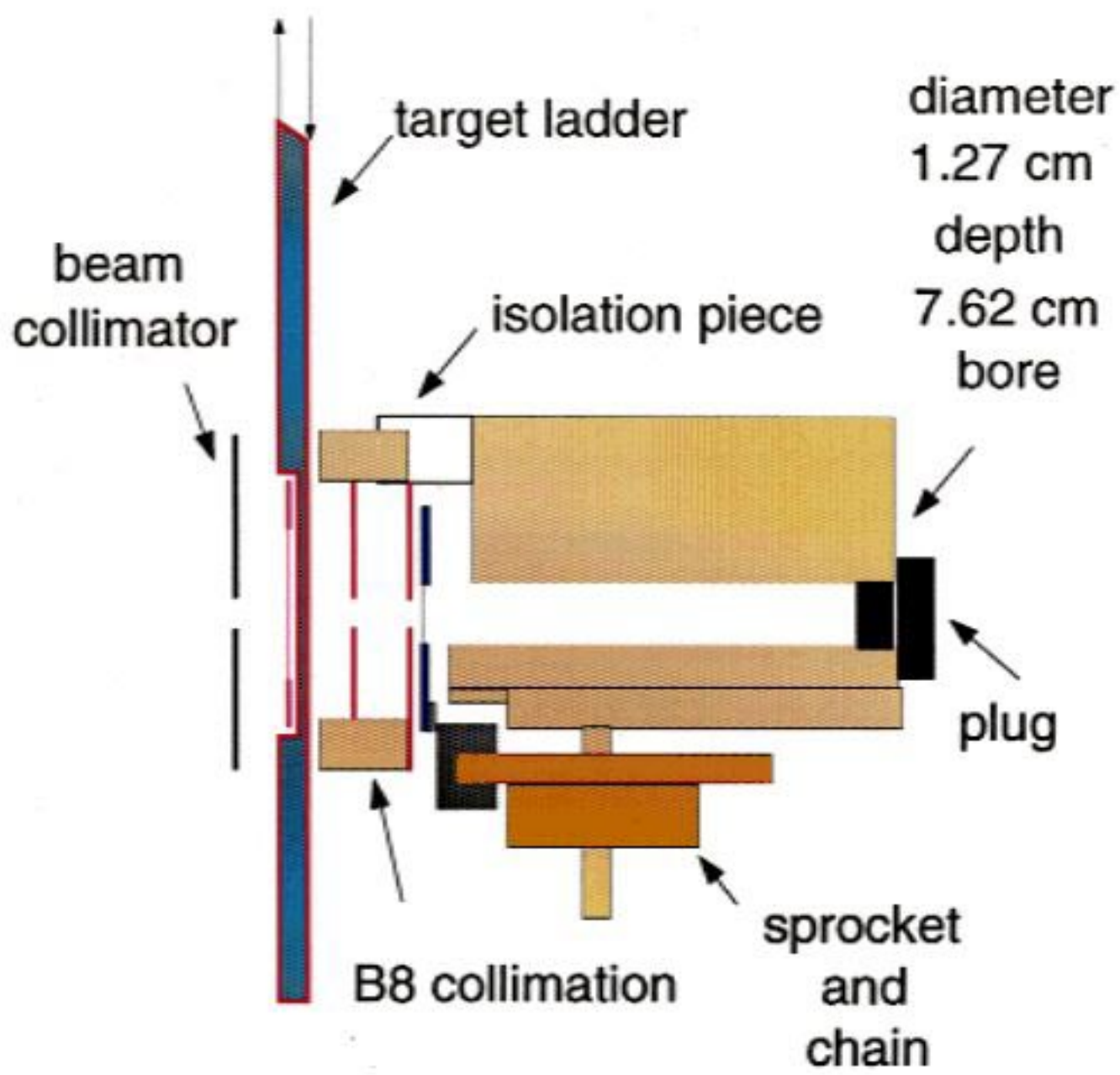
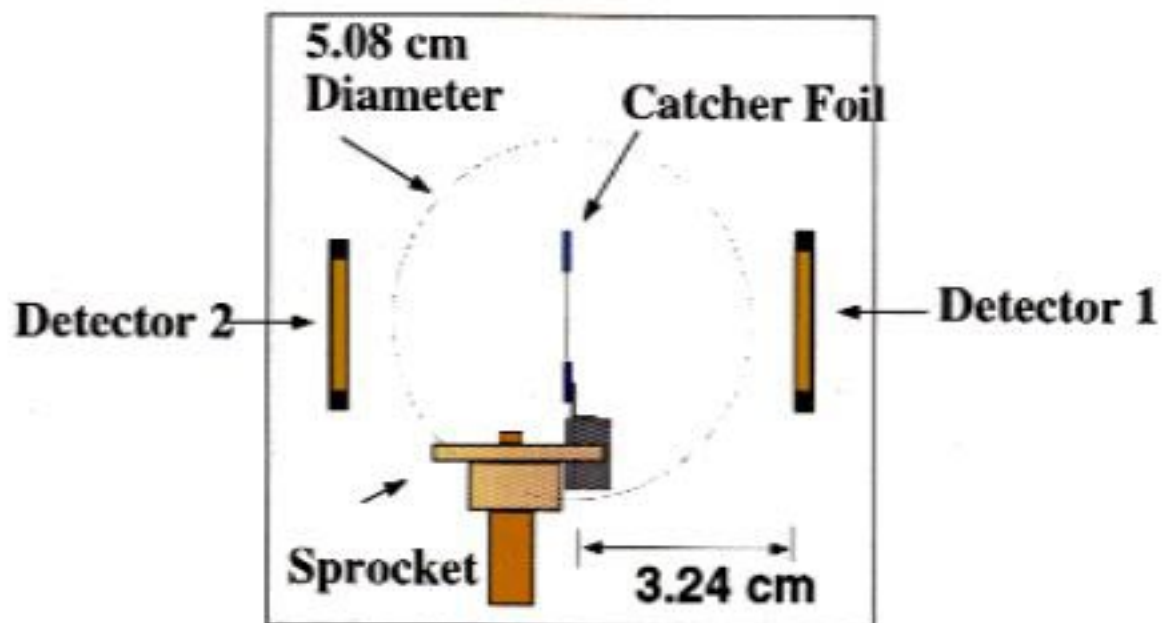


FIG. 5. The best-estimate (standard)  ${}^8\text{B}$  neutrino spectrum  $\lambda$ , together with the spectra  $\lambda^2$  allowed by the maximum ( $\pm 3\sigma$ ) theoretical and experimental uncertainties.

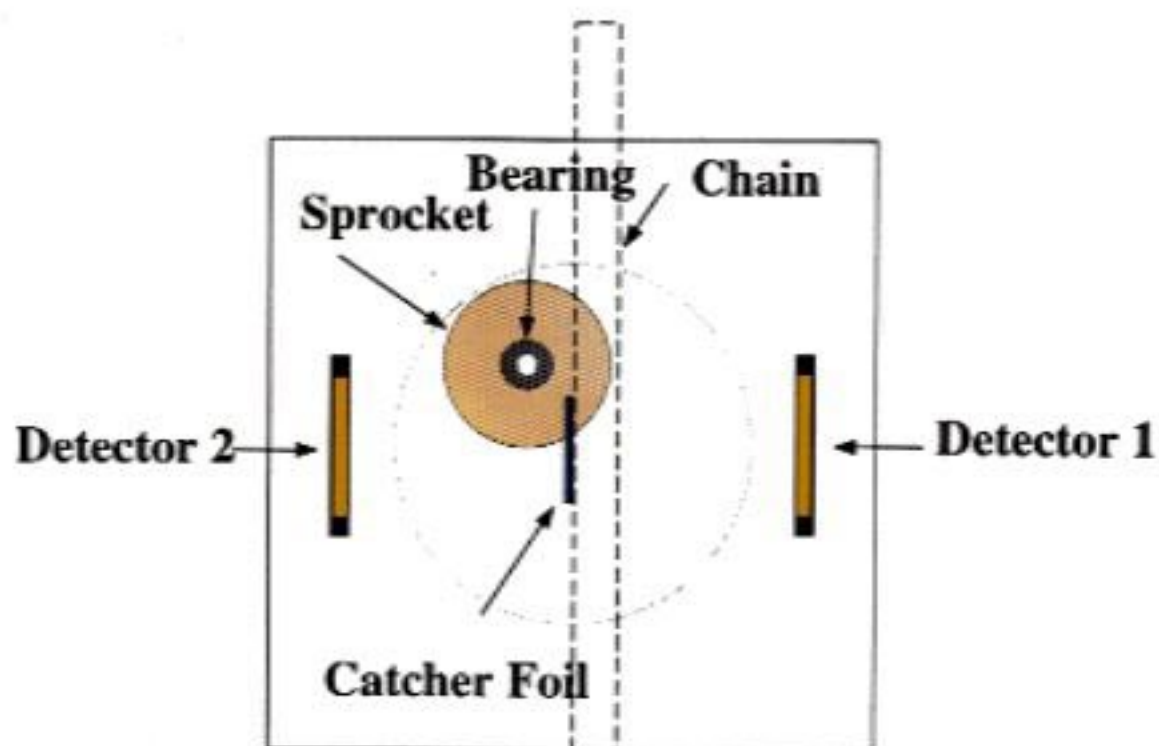
- pin diode detector
- catcher foil
- fixed Gd source
- mixed Gd & Am source
- plastic chain





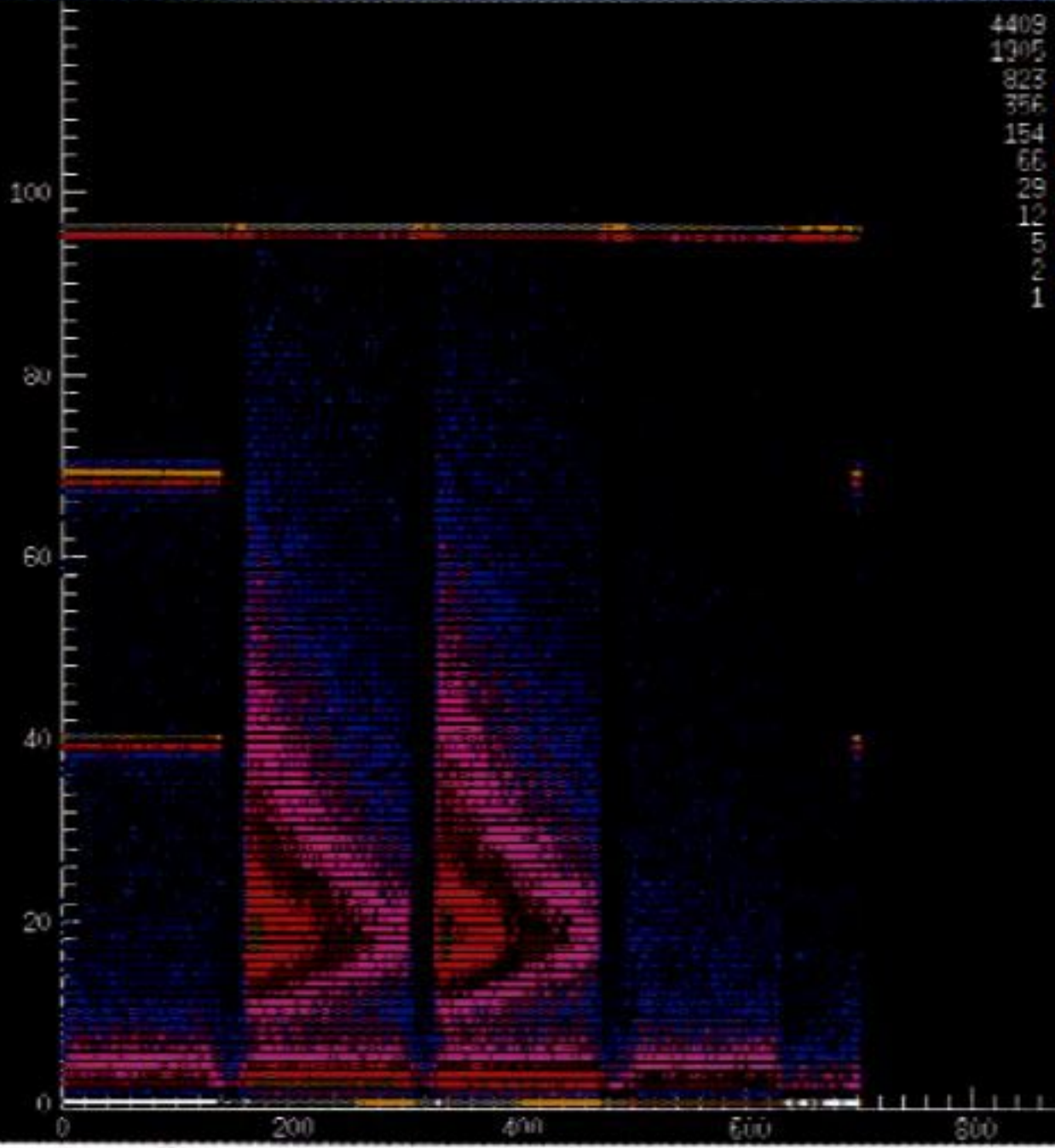


side view



overhead view

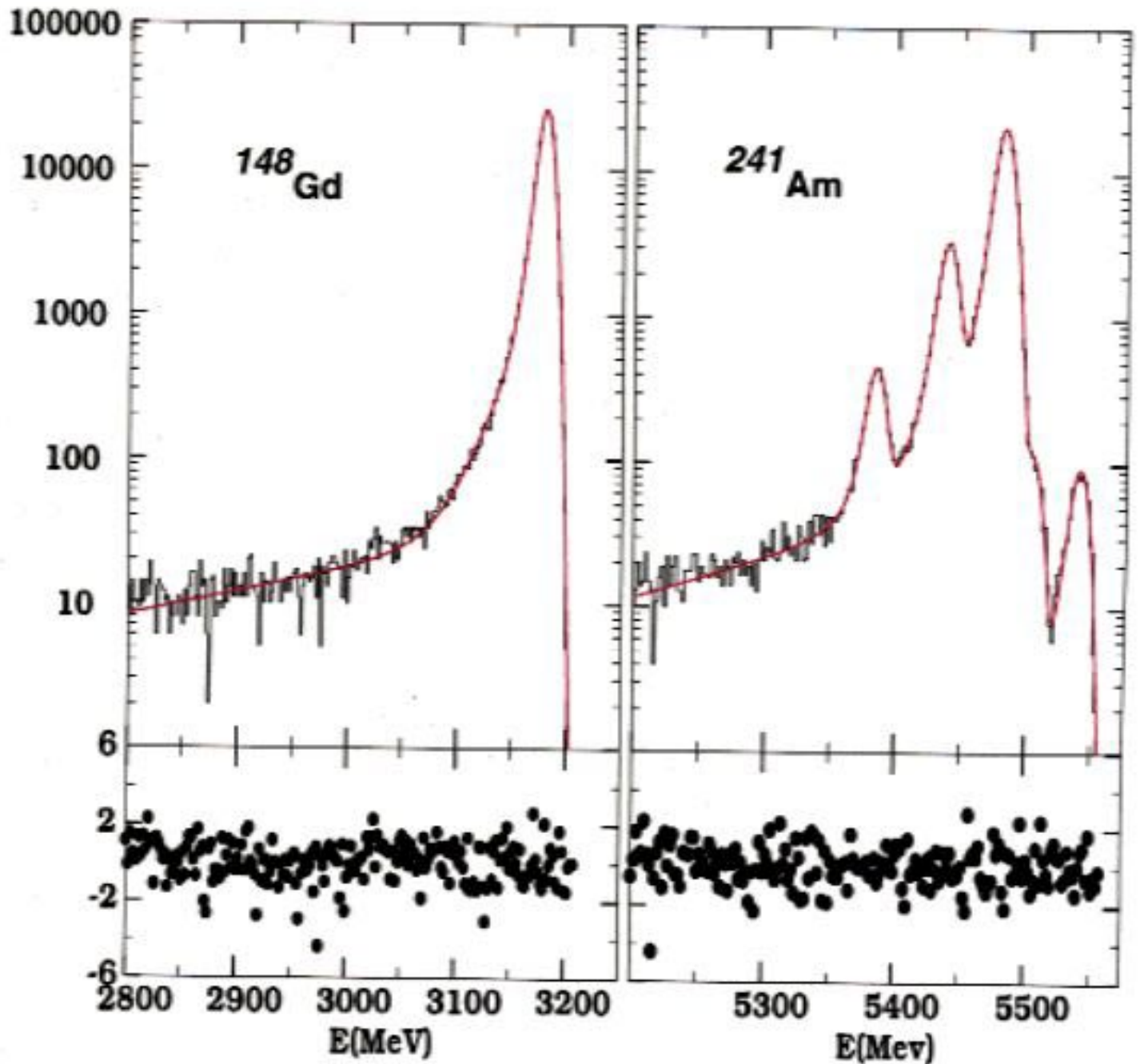
scan10\_13.his -ID=8- E2 Vs. Time



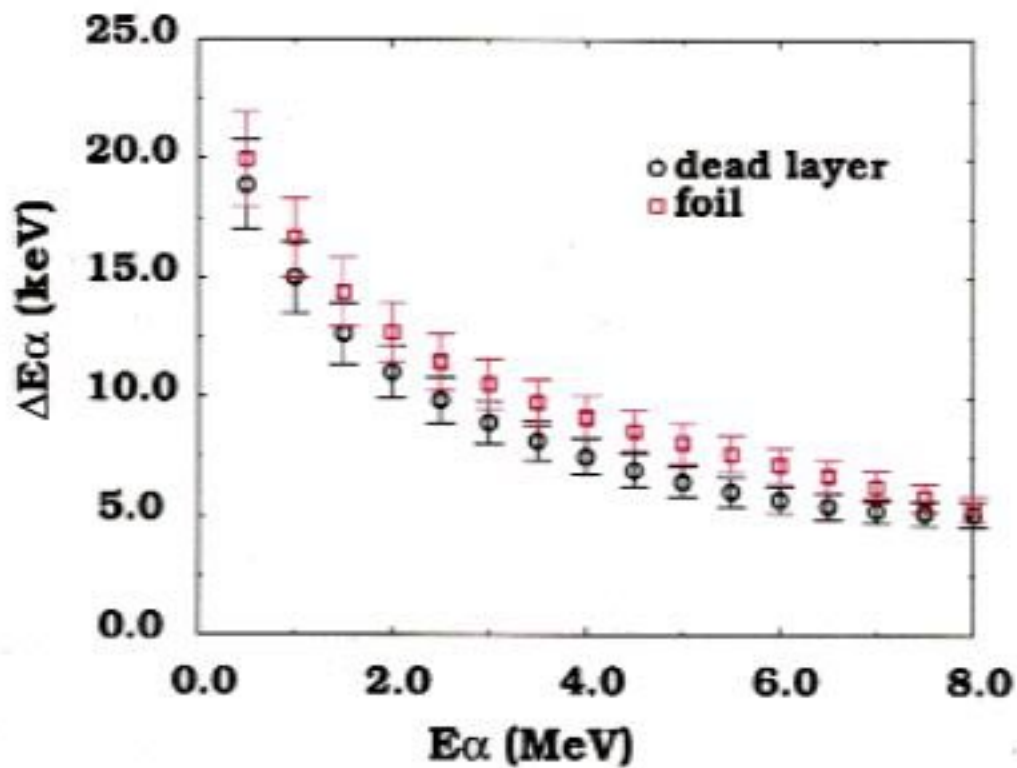
## Advantages of our Setup:

- 1) **Detectors completely blind to  $\beta$ 's**
  - a) allowed us to count  $\alpha$ - $\alpha$  coincidences without  $\beta$ 's.
  - b) cleared low-energy  $\beta$  backgrounds.
  - c) avoided  $\beta$  summing.
- 2) **Continuous  $\alpha$ -energy calibration.**
- 3) **Continuous foil-thickness monitoring.**

Energy calibrations are taken within each cycle in both detectors with mixed ( $^{148}\text{Gd}+^{241}\text{Am}$ ) sources

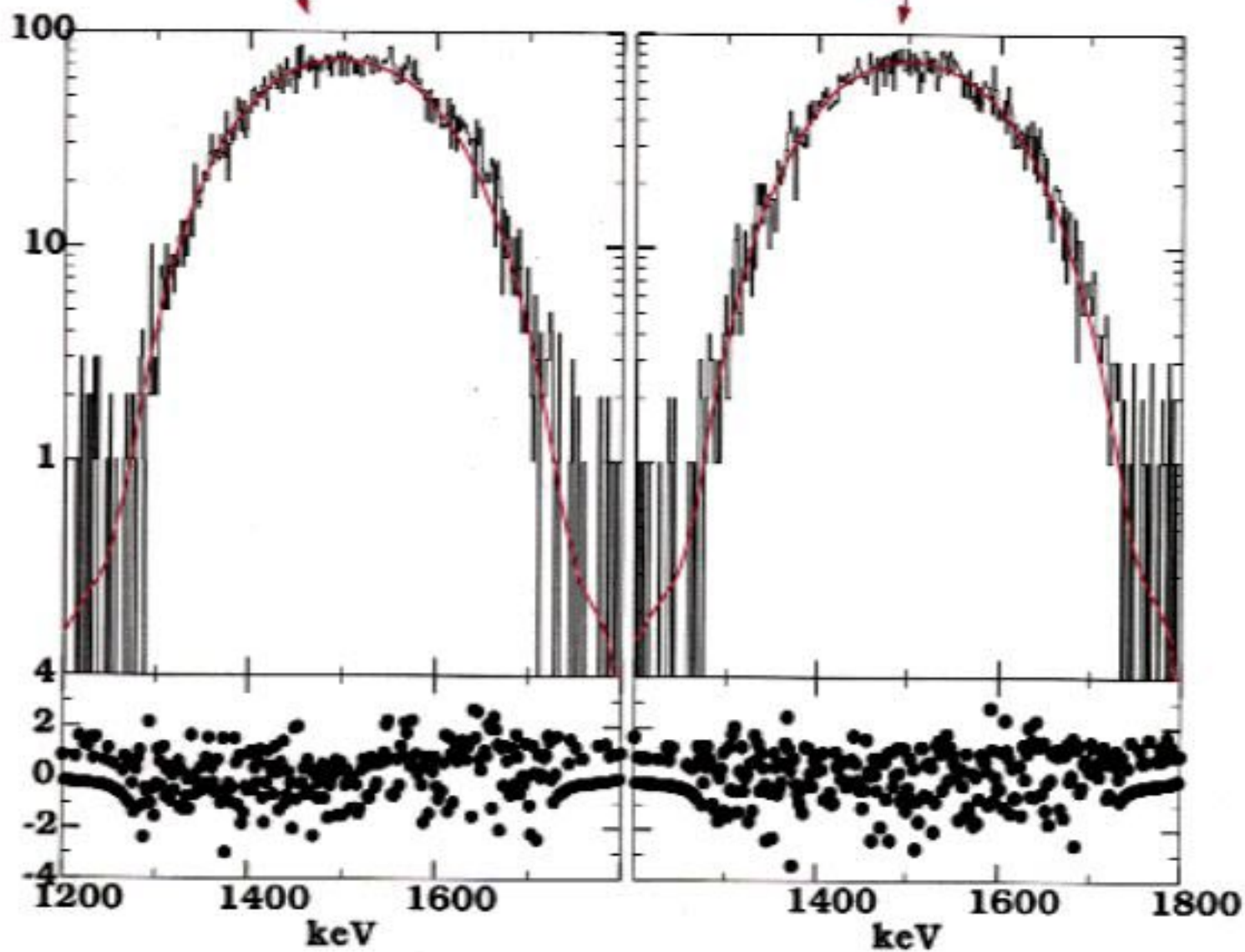
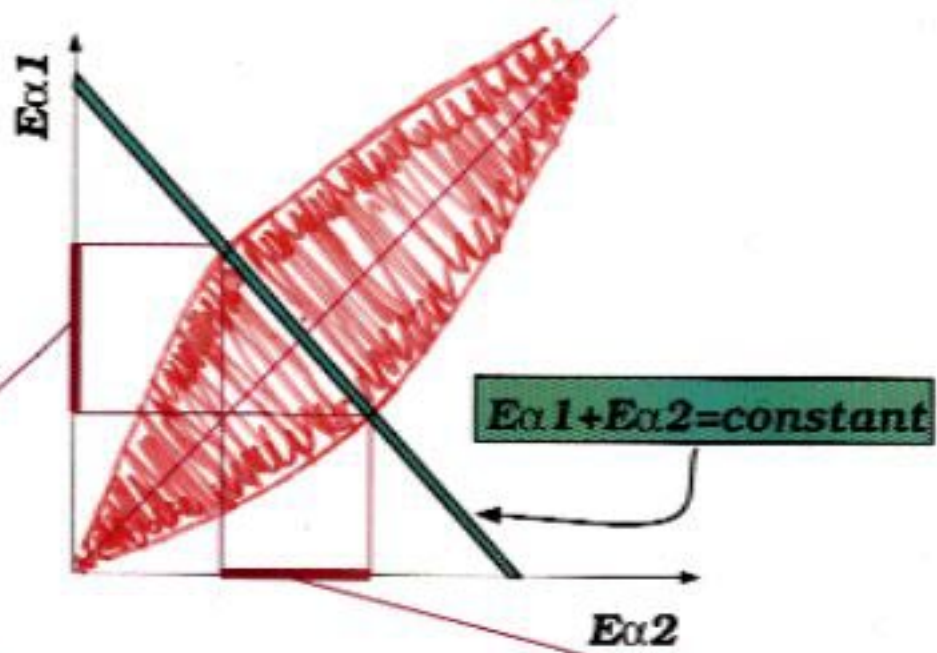


We measured detectors dead layers and calculated energy loss in the dead layers plus foils

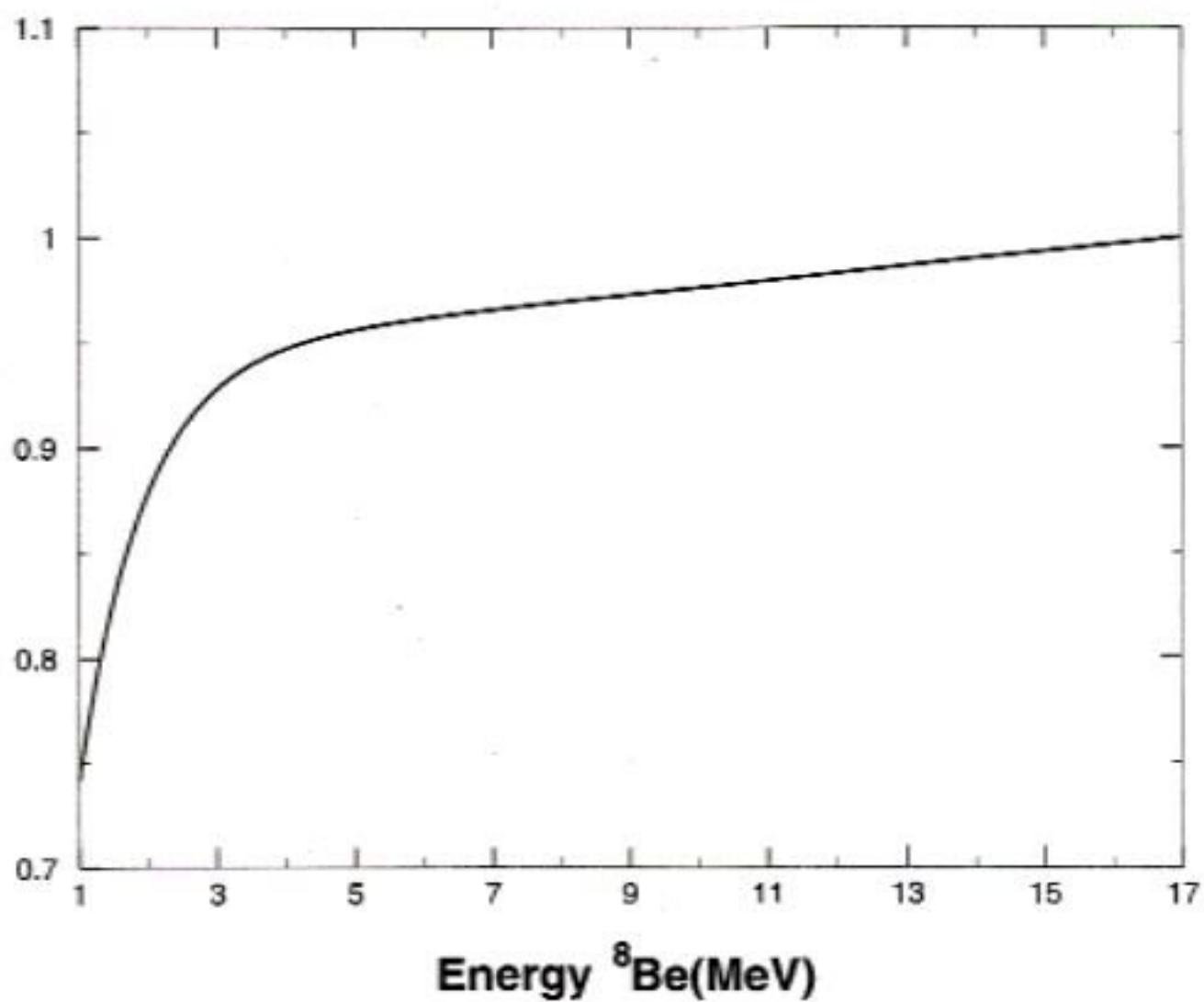


We corrected the 8B spectrum event-by-event for energy loss.





## Efficiency for ${}^8\text{B}$



The problem: 
$$-\frac{\hbar^2}{2m} \frac{d^2 \phi}{dr^2} + V(r) \phi = E \phi \quad (1)$$

Instead, we solve: 
$$-\frac{\hbar^2}{2m} \frac{d^2 X_\lambda}{dr^2} + V X_\lambda = E_\lambda X_\lambda \quad (2)$$

$$\left( \frac{dX_\lambda}{dr} + b X_\lambda \right)_{r=a} = 0$$

The solutions to the real problem can be expanded in terms of the  $X_\lambda$ 's:

$$\phi = \sum_\lambda A_\lambda X_\lambda$$

$$A_\lambda = \int_0^a X_\lambda \phi \, dr$$

From (1) and (2):

$$\frac{\hbar^2}{2m} \left( \phi \frac{dX_\lambda}{dr} - X_\lambda \frac{d\phi}{dr} \right) = (E - E_\lambda) A_\lambda$$

$$\phi(r) = G(r, a) \{ \phi'(a) + b \phi(a) \}$$

$$\Downarrow$$

$$\frac{\hbar^2}{2m} \sum_\lambda \frac{X_\lambda(r) X_\lambda(a)}{E_\lambda - E}$$

define "reduced width":  $\gamma_\lambda^2 = \frac{\hbar^2}{2m} [X_\lambda(a)]^2$

"R":  $R = \sum_\lambda \frac{\gamma_\lambda^2}{E_\lambda - E}$

To calculate cross section :

$$\phi_{\text{outside}} = I - U \phi \quad \left\{ \begin{array}{l} I = \frac{e^{-ikr}}{\sqrt{4\pi r}} \\ \phi = \frac{e^{+ikr}}{\sqrt{4\pi r}} \end{array} \right.$$

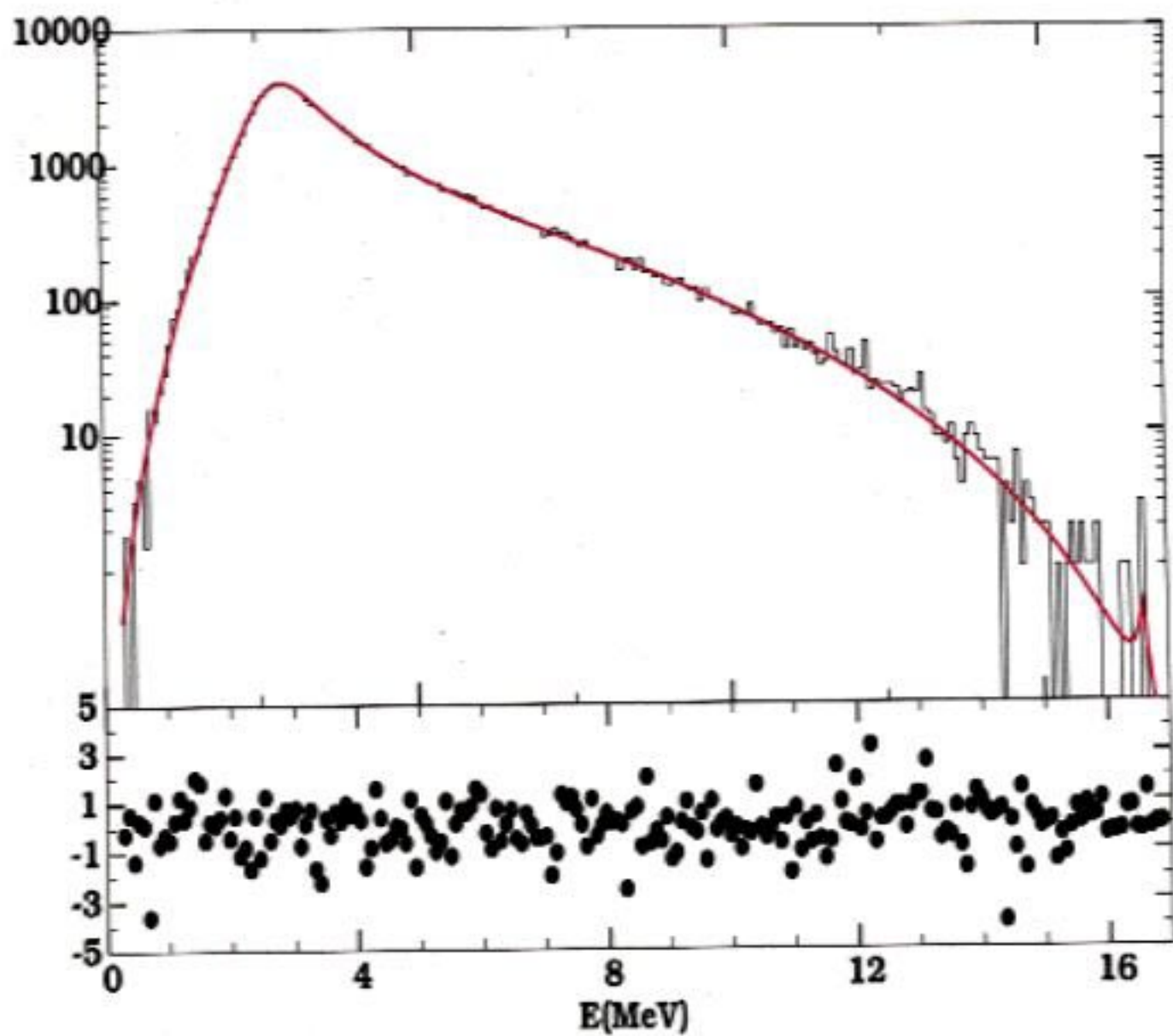
$$\sigma = \frac{\pi}{k^2} |1 - U|^2$$

To get  $U$  we take the logarithmic derivative and equate it to the value inside:

$$U = e^{-2ika} \frac{1 - bR + ikR}{1 - bR - ikR}$$

$$\Rightarrow \sigma = \frac{\pi}{k^2} \left| 2 \sin ka e^{ika} - \frac{2k\gamma_0^2}{(E_0 - E) - (b + ik)\gamma_0^2} \right|^2$$

## 8B energy spectrum



## R-matrix fit to the data

$$N(E) = \left( \frac{Nt}{6166\pi} \right) f_{\beta} P_2 \left( \frac{|\sum_{j=1}^n \frac{M_{Ej}\gamma_j}{E_j - E}|^2 + |\sum_{j=1}^n \frac{M_{Gj}\gamma_j}{E_j - E}|^2}{|1 - (S_2 - B_2 + iP_2) \sum_{j=1}^n \frac{\gamma_j^2}{E_j - E}|^2} \right) \quad (1)$$

The 16 MeV doublet was assumed to be a near equal mixture of  $T = 0$ , and  $T = 1$ . Let  $\psi_a$  and  $\psi_b$  be two wavefunctions with isospin 0 and 1, respectively:

$$\psi_2 = \alpha\psi_a + \beta\psi_b \quad , \quad \psi_3 = \beta\psi_a - \alpha\psi_b$$

The values of  $\alpha$  and  $\beta$  were extracted from the widths:

$$\alpha^2 = \frac{\Gamma_2}{\Gamma_0} \quad , \quad \beta^2 = \frac{\Gamma_3}{\Gamma_0} \quad , \quad \Gamma_0 = \Gamma_2 + \Gamma_3. \quad (2)$$

The relation between the reduced width  $\gamma_i$  and the width  $\Gamma_i$  for a given level were approximated by the following formulas

$$\gamma_1^2 = \frac{\Gamma_1}{2P_2(E_1) - \Gamma_1 \frac{dS_2(E_1)}{dE}} \quad , \quad \gamma_2^2 = \frac{\alpha^2 \Gamma_0}{2P_2(E_2)} \quad , \quad \gamma_3^2 = \frac{\beta^2 \Gamma_0}{2P_2(E_3)}. \quad (3)$$

The matrix elements for the 16 MeV doublet can then be expressed in terms of the matrix elements of the functions  $\psi_a$  and  $\psi_b$ .

$$M_{2T} = \beta M_{aT}$$

$$M_{3T} = -\alpha M_{bT}$$

$$M_{2GT} = \alpha M_{aGT} + \beta M_{bGT}$$

$$M_{3GT} = \beta M_{aGT} - \alpha M_{bGT}$$

$$M_{aT} = \sqrt{2}$$

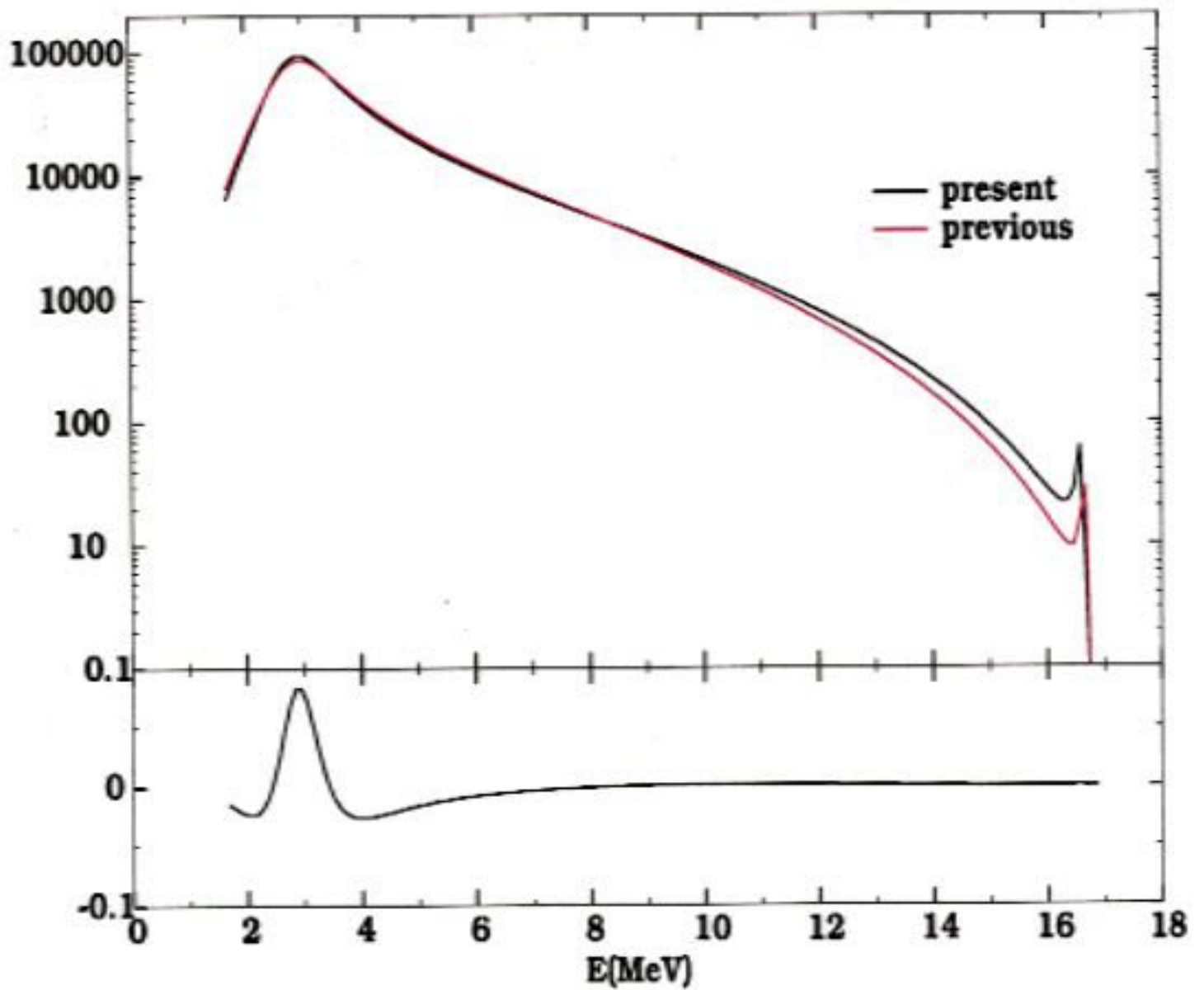
$$M_{bT} = 0$$

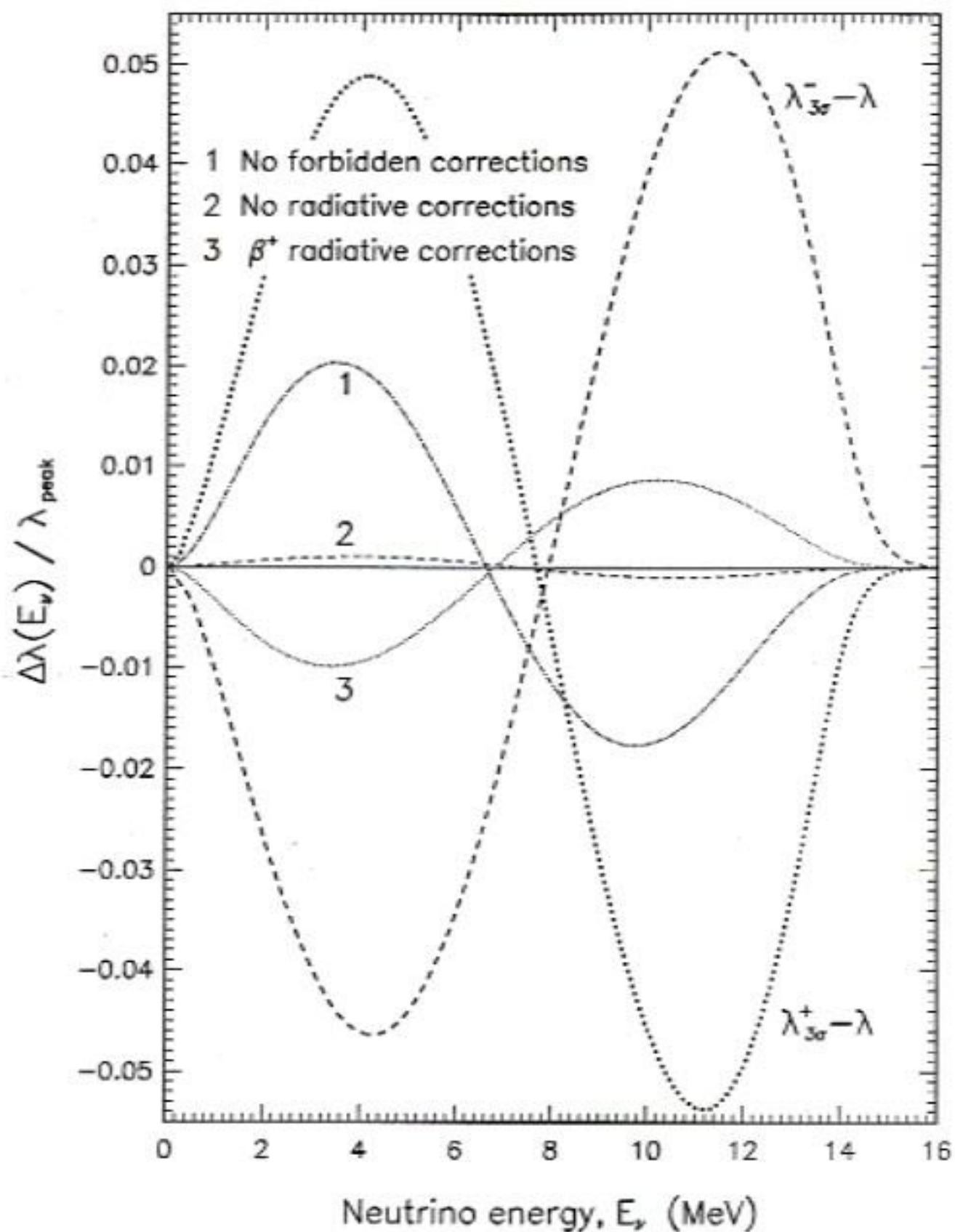
$$M_{aGT} = 0$$

$$M_{bGT} = 2.64$$

The value of  $M_{aGT}$  was left as a free variable in the  $\chi^2$  fit. It was also assumed that the contribution from  $M_{bGT}$  would not be significant and was held fixed at zero.

## **$^8\text{Be}$ endpoint distribution present results vs. previous results**







# Neutrino energy spectrum

